Atmos. Chem. Phys. Discuss., https://doi.org/10.5194/acp-2019-130
Manuscript under review for journal Atmos. Chem. Phys.
Discussion started: 25 March 2019

Atmospheric Chemistry and Physics
Discussions
Open Access

Biogenic and Anthropogenic sources of Arctic Aerosols

Ingeborg E. Nielsen[1,2], Henrik Skov[1,2,5], Andreas Massling[1,2], Axel C. Eriksson[3,4], Manuel Dall'Osto[6], Heikki Junninen[7,10], Nina Sarnela[7], Robert Lange[1,2], Sonya Collier[8], Qi Zhang[8], Christopher D. Cappa[9] and Jacob K. Nøjgaard[1,2]*

[1]Department of Environmental Science, Aarhus University, Roskilde, 4000, Roskilde, Denmark
[2]Arctic Research Centre, Aarhus University, Aarhus, 8000, Aarhus, Denmark
[3]Division of Ergonomics and Aerosol Technology, Lund University, Box 118, SE-22100, Lund, Sweden
[4]Division of Nuclear Physics, Lund University, Lund, Box 118, SE-22100, Lund, Sweden
[5]Institute of Chemical Engineering and Biotechnology and Environmental Technology, University of Southern Denmark, 5230, Odense, Denmark
[6]Institute of Marine Sciences, CSIC, Passeig Marítim de la Barceloneta, 37-49. E-08003, Barcelona, Spain
[7]Institute for Atmospheric and Earth System Research / Physics, Faculty of Science, University of Helsinki, 00140 Helsinki, Finland
[8]Department of Environmental Toxicology, University of California, Davis, CA 95616, USA
[9]Department of Civil and Environmental Engineering, University of California, Davis, CA 95616, USA
[10]Institute of Physics, University of Tartu, Ülikooli 18, EE-50090 Tartu, Estonia

Correspondence to: Ingeborg Elbæk Nielsen (ien@envs.au.dk)

Abstract. There are limited measurements of the chemical composition, abundance, and sources of black carbon (BC) containing particles in the high Arctic. To address this, we report 93 days of Soot Particle Aerosol Mass Spectrometer (SP-AMS) data collected in the high Arctic. The period ~~spans from~~ February 20th until May 23rd 2015 at Villum Research Station (VRS) in Northern Greenland (81°36' N). Particulate sulfate (SO_4^{2-}) accounted for 66% of the non-refractory PM_1, which amounted to 2.3 µg m^{-3} as an average value observed during the campaign. The second most abundant species was organic matter (24%), averaging 0.55 µg m^{-3}. Both organic aerosol (OA) and PM_1, estimated from the sum of all collected species, showed a marked decrease throughout May in accordance with Arctic haze ~~leveling off~~. The refractory black carbon (rBC) concentration averaged 0.1 µg m^{-3} over the entire campaign.

Positive Matrix Factorization (PMF) of the OA mass spectra yielded three factors: (1) a Hydrocarbon-like Organic Aerosol (HOA) factor, which was dominated by primary aerosols and accounted for 12% of OA mass; (2) an Arctic haze Organic Aerosol (AOA) factor, which accounted for 64% of the OA and dominated until mid-April while being nearly absent from the end of May; and (3) a more oxygenated Marine Organic Aerosol (MOA) factor, which accounted for 22% of OA. AOA correlated significantly with SO_4^{2-}, suggesting the main part of that factor being secondary OA. The MOA emerged ~~late~~ at the end of March, where it increased with solar radiation and reduced sea ice extent, and dominated OA for the rest of the campaign until the end of May. ~~Important differences are observed among the factors, including~~ the highest O/C ratio (0.95) and S/C ratio (0.011) ~~for~~ MOA ~~– the marine related factor~~. Our data supports current understanding of the Arctic summer aerosols, driven mainly by secondary aerosol formation, but with an important contribution from marine emissions. In view of a changing Arctic climate with changing sea-ice extent, biogenic processes, and corresponding source strengths, highly

time-resolved data are urgently needed in order to elucidate the components dominating aerosol concentrations.

1 Introduction

Climate change driven by anthropogenic emission of greenhouse gases seriously impacts the Arctic. Areas such as the Arctic have experienced average temperature increases of twice the global mean during the last 100 years (IPCC, 2013). Warming has led to destabilization of permafrost (AMAP, 2017) and a longer melting season resulting in a critical decrease in the sea-ice extent (Stroeve et al., 2007). The latter changes the Earth’s albedo and results in positive sea-ice and snow-albedo feedbacks causing further warming (Lenton, 2012). In addition to long-lived greenhouse gases such as CO_2, atmospheric aerosols also have an impact on the radiation balance of the Earth. Aerosols affect the radiative balance in various ways. They can absorb and scatter solar radiation, causing either warming or cooling of the atmosphere, respectively. Aerosols can also impact the properties of clouds, for example affecting cloud reflectivity, by serving as cloud ~~and ice-condensation nuclei~~ (Twomey, 1977).

It is well established that the aerosol concentration in the Arctic atmosphere is seasonally varying resulting in higher loadings during winter and spring, compared to summer and fall, often referred to as “~~the~~ Arctic haze” (Heidam et al., 2004; Tunved et al., 2013; Heidam et al., 1999; Quinn et al., 2007; Barrie et al., 1981; Heidam, 1984). This is explained by a greater accessibility to the lower troposphere in the Arctic from anthropogenic source regions outside the Arctic due to an expansion of the polar dome (AMAP, 2011) in winter and spring. In addition, during the Arctic winter strong temperature inversions create stable stratification where aerosol removal processes are strongly reduced prolonging their atmospheric lifetime (Stohl, 2006; Sodemann et al., 2011; AMAP, 2011). The air masses inside the wintertime dome are extremely dry, limiting aerosol wet deposition, while low turbulence ~~exchange~~ caused by the stratification and slow vertical exchange reduces the dry deposition of aerosols (Sodemann et al., 2011; Stohl, 2006; Abbatt et al., 2018). The Arctic haze is observed during spring and is visible as a distinct pollution layer (Heidam et al., 1999; Law and Stohl, 2007; Stohl, 2006; Heidam et al., 2004). Arctic haze particles effectively scatter light (Andrews et al., 2011; Schmeisser et al., 2018), and act as cloud condensation nuclei (CCN) (Earle et al., 2011; Komppula et al., 2005). A major part of the aerosol mass is long-range transport from source regions outside the Arctic where the primary source region has been identified as the northern part of Eurasia (Nguyen et al., 2013; Quinn et al., 2008; Heidam et al., 2004; Stohl et al., 2007; Abbatt et al., 2018; Christensen, 1997). Studies have shown that main constituents of Arctic aerosols are sulfate (SO_4^{2-}) and organics mixed with a minor fraction of nitrate (NO_3^-), ammonium (NH_4^+), black carbon (BC) and heavy metals (Quinn et al., 2007; Fenger et al., 2013; Nguyen et al., 2013; Frossard et al., 2011; Barrie et al., 1981). This is also the case at the high Arctic station, Villum Research Station (VRS) at Station Nord in North Greenland, where this study was conducted. Rahn and Heidam (1981) have previously estimated the average chemical composition of Arctic submicrometer aerosols during winter-spring, ~~which amounted to~~ 2 µg m^{-3} SO_4^{2-}, 1 µg m^{-3} organic aerosol (OA), 0.3-0.5 µg m^{-3} BC and a few hundred ng m^{-3} of other compounds. Since then, SO_4^{2-} and BC during winter-spring have declined at Alert, Mount Zeppelin and VRS (Heidam et al., 1999; Hirdman et al., 2010). However, the total Arctic column burden may have increased (Sharma et al., 2013). No significant changes have been observed for SO_4^{2-} and BC at Barrow (Hirdman et al., 2010).

BC is the most important aerosol ~~at~~ absorbing solar radiation in the atmosphere. Of particular concern for the Arctic, ~~when~~ BC ~~is deposited~~ on snow and ice-covered surfaces it changes the albedo, lead~~ing~~ to increased absorption of solar radiation and direct heating of the surface (Bond et al., 2013). Consequently, melting accelerates giving BC an important role especially in an Arctic context (Bond et al., 2013; Quinn et al., 2008; AMAP, 2011). Long-range transport of BC to the Arctic is very effective in mid-winter, when removal processes are slowest. Transport reaches a minimum in March – April and wet deposition becomes the most important removal process in the later spring (Abbatt et al., 2018). Still, natural emissions from vegetation fires can be considerable in spring and early summer (Mahmood et al., 2016). Overall, this leads to a general seasonal cycle with the highest concentrations of BC observed between January and April and the lowest concentrations throughout the summer, but with periodic spikes in concentration throughout the summer (Sharma et al., 2006). OA is also an important component of Arctic aerosol and is composed of many different molecules derived from either primary emissions or from secondary production. Consequently, there are often many distinct sources of OA. OA can typically contribute up to one third of PM_1 in the Arctic though few studies have characterized this component in detail (Ba[illegible] et al., 2015; Brock et al., 2011; Frossard et al., 2011; Kawamura et al., 2010; Quinn et al., 2002; Shaw et al., 2010). Total OC is relatively constant or decreasing with time in late winter. However, during spring it increases suggesting that there is photochemical production of OA (Willis et al., 2018). There is a need for more detailed measurements of OA composition in the Arctic to better understand the key sources and how these vary with time (Willis et al., 2018). Due to aerosols' climatic importance it is crucial to expand the knowledge regarding their chemical and physical properties in the Arctic to reduce the current uncertainty (IPCC, 2013) with respect to the overall effect of aerosols on Earth's energy budget.

It is crucial to understand natural sources in addition to anthropogenic sources of Arctic aerosols. Marine and coastal marine locations constitue a large part of Arctic, and marine aerosols ~~is~~ a source of inorganic and organic aerosols. Production of primary marine aerosols is known to correlate with wind speed and possibly also other mechanisms (Willis et al., 2018). Primary marine organic aerosols in Arctic regions are believed to consist of water soluble or surface active organic compounds present in the surface water, or water insoluble microgels (Willis et al., 2018; Leck and Bigg, 2005; Orellana et al., 2011). Sea salt aerosols play an important role for the climate in spring and autumn (Abbatt et al., 2018). Methane sulfonic acid (MSA), an oxidation product of dimethyl sulfide (DMS) is abundant in spring and summer (Abbatt et al., 2018) and is a key indicator of secondary marine aerosols. Increases in MSA levels has been associated with marginal sea ice moving North (Laing et al., 2013; Quinn et al., 2009; Sharma et al., 2012). In fact, DMS emissions in the Arctic have increased by 30% per decade the last two decades due to both increased temperatures and decreased ice cover (Abbatt et al., 2018). A relationship between MSA and the frequency of new particle formation has also been recently ~~demonstrated~~ based on long-term observations (Dall'Osto et al., 2017). This suggest that DMS is important for summertime particle ~~formation.~~ Another important natural source of Arctic aerosols is ammonia, which ~~is believed~~ to originate from migrating sea bird colonies (Croft et al., 2016). Modeling studies have been shown to better capture particle burst and growth when an ammonia source from sea birds were included (Croft et al., 2018; Croft et al., 2016). Additionally, ammonia can also be transported from boreal wildfires from lower latitudes.

Many previous Arctic studies have been based on off-line analysis and filter measurements of ambient aerosols with a relatively low time resolution of hours up to a week (Heidam et al., 1999; Heidam et al., 2004; Skov et al., 2006; Quinn et al., 2007; Massling et al., 2015; Leaitch et al., 2018; Sharma et al., 2012; Quinn et al., 2009). Beside the low time resolution, two disadvantages of these types of measurements can be evaporate loss or adsorption of semi-volatile compounds (Lee et al., 2013; Dillner et al., 2009). Highly time-resolved in-situ measurements can reduce these artifacts while ~~also enabling the possibility to observe~~ the variations ~~and trends~~ of different chemical species on a much shorter time-scale. In this way, it is possible to ~~look into the processes behind the observed levels~~. In the last decade, ~~Aerosol Mass Spectrometr~~ (AMS) (Canagaratna et al., 2007; DeCarlo et al., 2006; Jimenez et al., 2003; Drewnick et al., 2005; Jay al., 2000) has been widely used as an on-line method for quantitative analysis of chemical composition of atmospheric particles. With the addition of a laser vaporizer (Onasch et al., 2012), its application has been extended to include refractory aerosol components, including refractory black carbon (rBC).

In this study, the time dependent concentrations of sub-micrometer particle composition including OA, SO_4^{2-}, NO_3^-, NH_4^+, chloride (Cl) and rBC are reported ~~at~~ the high Arctic site VRS in Northern Greenland. The measurements were conducted ~~by application of~~ a soot particle aerosol mass spectrometer (SP-AMS) and auxiliary measurements during the Arctic spring 2015, when concentrations are expected to peak. This study presents three months of data using an SP-AMS in the high Arctic. The objectives are to gain better insight into the processes influencing the chemical composition of high Arctic aerosols and to allocate potential sources and source regions. The ~~latte~~ s investigated through positive matrix factorization (PMF) of the organic aerosol mass spectra fr e SP-AMS.

2 Experimental

2.1 Sampling site

The atmospheric measurements were carried out at VRS located at the Danish military station, Station Nord in North Greenland (Figure S1, 81^0 36'N, 16^0 40'W, 24 m above mean sea level). VRS is situated in a region with a dry and cold climate where the annual precipitation is 188 mm and the annual mean temperature is -21 °C. The dominating wind direction is southwestern with an average wind speed of 4 m s^{-1} as apparent from Figure S1 (Rasch et al., 2016; Nguyen et al., 2013). The SP-AMS data were sampled in an atmospheric observatory containing two laboratories whereas data from a multi-angle absorption photometer (MAAP) and a filter pack sampler ~~was~~ collected in a smaller co-located hut (Flygers hut) - both equipped with particle and gas inlets. The two measurement sites are located 2.5 km southeast of the military station and are only 300 meters apart. Given the close proximity of the two laboratories and the lack of ~~hyper-~~local sources, we expect both to sample largely the same air mass. A high-volume sampler (HVS) provided filter samples for off-line analysis. The HVS was located at the outskirts of the military station, hence 2.5 km from the main sampling site. All particulate measurements in the Atmospheric Observatory were conducted by drawing air through a slightly heated (absolute 5 °C) particle inlet custom-built by TROPOS. Sampling took place during a campaign within CRAICC (Cryosphere-Atmosphere Interactions in a Changing Arctic Climate) and extended over a three months period from 20 February until 23 May 2015.

2.2 The soot-particle aerosol mass spectrometer

An SP-AMS (Aerodyne Research Inc.) was deployed at VRS for measuring mass concentration and chemical composition of submicrometer aerosols with a time resolution of two minutes. The SP-AMS is described in detail elsewhere (Onasch et al., 2012). In brief, the instrument samples aerosols into a vacuum chamber through an aerodynamic particle lens, which creates a narrow particle beam. In the vacuum chamber, the aerosols accelerate to a velocity depending on their vacuum aerodynamic diameter enabling analysis of the aerosol size distribution. Subsequently, the aerosols undergo vaporization, ionization with 70 eV electron impact, and detection with time-of-flight mass spectrometr~~y~~. The vaporization in the SP-AMS can occur in two ways: (1) impaction on a tungsten surface at a temperature of 600 °C, or (2) intersection with the beam of a continuous-wave 1064 nm intracavity Nd:YAG laser. The laser extends the application of the AMS to include refractory particulate matter (R-PM) since it enables vaporization of strongly infrared light absorbing particles, such as refractory BC (Onasch et al., 2012). In this study, high-resolution (HR) mass concentrations of SO_4^{2-}, NO_3^-, NH_4^+, organics, Cl and rBC are obtained from the SP-AMS.

The SP-AMS was operated in two minutes laser off and two minutes laser on in V-mode and alternated between the mass spectrum mode and the particle time-of-flight (pToF) to obtain submicrometer particle~~s~~ (PM_1) ~~and particle size distribution, respectively~~. Non-refractory species are reported for time periods where the laser was off. The flow rate was inspected with a Gilian Gilibrator (Sensidyne) and pToF size calibration with ammonium nitrate particles was performed at the beginning and at the end of the field study. During the first part of the campaign, ionization efficiency (IE) calibrations with ammonium nitrate particles were conducted on a weekly basis and during the last part every second week. To establish the detection limit and to enable adjustments of the fragmentation table~~s~~ a high-efficiency particulate air (HEPA) filter was applied on a daily basis for a period of 30 to 60 minutes with a time resolution of 2 minutes. The lower detection limit of the different species was determined as three times the standard deviation of the mass concentration during the HEPA filter periods (Table 1). The data were analyzed with the standard AMS Igor Pro-based (version 6.35 Wavemetrics, Inc) software tools SQUIRREL (version 1.57G) and PIKA (version 1.16H), available at http://cires1.colorado.edu/jimenez-group/ToFAMSResources/ToFSoftware/index.html. The analysis followed the principles described in DeCarlo et al. (2006), Jimenez et al. (2003); Allan et al. (2004) and Onasch et al. (2012).

The default relative ionization efficiency (RIE) values for OA, SO_4^{2-}, NO_3^-, NH_4^+ and Cl of 1.4, 1.2, 1.1, 4 and 1.3, respectively, were applied, which are based on Canagaratna et al. (2007). It should be noted that chloride reported in the current study is measured with laser off and is thus non-refractory chloride and largely excludes refractory species such as chloride in sea salt aerosols. Thus, reported Cl in this study is most likely primarily a sum of organic Cl and NH_4Cl due to the acidic environment at VRS. However, the partitioning of chloride between different specices has not been investigated further, since it is not within the scope of this study. A RIE for rBC of 0.46 was found from calibrations with Regal Black (a commercial carbon black). The appropriateness of this RIE for ambient Arctic rBC is discussed further below (Section 2.4). Calibrations with Regal Black and ammonium nitrate were done with the same frequency. Fragment ions from organic species can overlap with some of the marker ions for rBC. To minimize the organic contribution to the nominal rBC signal (especially at C_1^+ an organic contribution was evident), C_3^+ was used to quantify rBC. Thus, the C_3^+ signal was scaled with a factor of 1/0.55 to match the fraction in the Regal Black mass spectra (Martinsson et al., 2015). The applied collection efficiency (CE) for non-refractory PM and rBC will be discussed in more detail in a subsequent section.

2.3 Auxiliary equipment

The aerosol light absorption was measured using a MAAP (Model 5012 Thermo Scientific) operated at a flow rate of 1 m^3 $hour^{-1}$ with an inlet without a size cut-off. Aerosols were sampled on a filter in which the light absorption at 670 nm was measured by a photometer. Detailed information about the instrument can be found in Petzold and Schonlinner (2004) and previous MAAP measurements from VRS are published in Massling et al. (2015). The BC concentration is determined from the relationship between the aerosol light absorption coefficient and a specific aerosol absorption coefficient (Petzold and Schonlinner, 2004). The specific absorption coefficient describes BCs ability to absorb solar radiation at a specific wavelength, which depends on the age of the aerosol (Petzold et al., 1997; Sharma et al., 2002) and is often determined based on correlations with thermal-optical measurements of elemental carbon (EC) (Sharma et al., 2004). In this study, the MAAP's default value of 6.6 m^2/g has been applied based on Massling et al. (2015). Uncertainty in the conversion factor likely impacts the reported absolute concentrations, but not the temporal variability. In addition, a scanning mobility particle sizer (SMPS) measured the particle number size distribution, which was used for validating the SP-AMS results. Description of validation can be found in Supporting Information.

2.4 Comparison between instruments

A collection efficiency (CE) adjustment is normally applied to AMS data, which accounts for particle loss in the instrument caused by the inlet and the aerodynamic lens, beam divergence, and particle bounce effects (Canagaratna et al., 2007; Onasch et al., 2012). In this study, the parameterization developed by Middlebrook et al. (2012) has been used where a time dependent CE is determined based on the aerosols chemical composition. Previous studies have shown an increasing CE with particle acidity, the content of nitrate, and relative humidity (Quinn et al., 2006; Jayne et al., 2000; Matthew et al., 2008). The time dependent CE varied with the majority of values between 0.8 and 1 (Figure S2). In this study, the high CE was due to acidic aerosols. This is also evident from Figure S3.a showing that the theoretical predicted NH_4^+ concentration necessary for neutralizing the mass concentration of inorganic anions is much larger than the actual NH_4^+ concentration measured by the SP-AMS (slope = 0.15). The acidity is explained by the high amount of sulfuric acid.

Atmos. Chem. Phys. Discuss., https://doi.org/10.5194/acp-2019-130
Manuscript under review for journal Atmos. Chem. Phys.
Discussion started: 25 March 2019

Applying the RIE for rBC of 0.46 determined from Regal Black calibrations, a good correlation between rBC and BC_{MAAP} is found (Figure S3.b). While there is a strong linear relationship between the two (R^2 = 0.83), the BC_{MAAP} was about three times ~~larger~~ than the SP-AMS rBC (slope = 0.33 ± 0.02). This indicates that the actual RIE for rBC was lower than the value of 0.46 determined during laboratory calibrations. A lower RIE can be explained by different particle size and a more complex morphology of the Arctic soot compared to the Regal Black used for calibration. An effective RIE is determined for rBC by forcing the SP-AMS measurements to match the MAAP measurements. For rBC an effective RIE of 0.15 (= 0.33 * 0.46) is hence applied in this study.

Comparison of the total PM_1 mass concentration (sum of OA, SO_4^{2-}, NH_4^+, NO_3^-, Cl and rBC) with the calculated total volume from the SMPS assuming spherical particles was carried out to validate the SP-AMS results. The SMPS was operated to characterize particles having mobility diameters between 9 and 870 nm. This corresponds to a larger size range than sampled by the SP-AMS, which has 100 % transmission efficiency within aerodynamic diameters between 70 and 600 nm, and adjustment from aerodynamic diameter to mobility diameter further brings the SP-AMS into the SMPS range (DeCarlo et al., 2006; Allan et al., 2003). However, previous studies (Nguyen et al., 2016; Lange et al., 2018) have shown that the dominant particle size range at VRS during winter and spring months is within detection range of the SP-AMS. Thus, the number of particles from the SMPS exceeding the size ~~span~~ measured by the SP-AMS should be relatively small and thereby not influence the results, since particles in the lower end of the size distribution do not significantly contribute to volume. There was a generally reasonable temporal correspondence between the two measurements. Although there were some periods where they differed notably ~~it~~ were within the expected range given the accuracy of the two instruments. A more detailed discussion about the comparison between the two instruments is presented in Supporting Information (Figure S5).

2.5 Positive Matrix Factorization

PMF analysis (Paatero, 1997; Paatero and Tapper, 1994; Lanz et al., 2007; Ulbrich et al., 2009) was conducted on the organic mass spectra time dependent concentration to determine OA factors, which can be linked to the different sources of OA. The analysis was carried out with the PMF Evaluation Tool Software (PET, v2.08D; available online at http://cires1.colorado.edu/jimenez-group/wiki/index.php/PMF-AMS_Analysis_Guide) on ~~a~~ mass spectra consisting of HR ions with *m/z* values from 12 to 100. The detailed procedure is described elsewhere (Ulbrich et al., 2009; Zhang et al., 2011). The input HR mass spectra and error matrix with the appropriate ion fragments were generated in PIKA, where the error matrix was calculated as the sum of the quadrature of the electronic noise and Poisson counting for each ion (Allan et al., 2003). Isotopes were removed from both the data and error matrix since they would give additional weight to the parent ion in the PMF analysis.

As described in Ulbrich et al. (2009) "weak" ions with a signal-to-noise ratio (SNR) between 0.2 and 2 were down-weighted by a factor of 2 whereas "bad" ions with a SNR below 0.2 were removed from the data and error matrix. The PMF was executed in exploration mode with a range of factors (between 1 and 5). The robustness of the solutions were tested by setting different random starting points (SEED: 0

to 10, steps = 1) (Zhang et al., 2011). The detailed procedures for choosing the best solution were based on Zhang et al. (2011). A solution with three factors was identified after evaluating Q/Q_{exp} and residuals, interpreting the mass spectra and investigating the temporal correlation between the factor time series and potential tracer species (Ulbrich et al., 2009; Zhang et al., 2011). FPEAK and seed values were changed to test the stability of the three-factor solution and based on the diagnostic plots a three-factor solution was selected with a FPEAK and seed value of zero (Figure S7). A 4-factor solution was scientifically not meaningful with respect to chemistry and returned an O/C ratio >> 1 for one of the factors. Hence we do not observe a fourth "continental" factor, which has been previously observed during the ASCOS cruise track in the summer/autumn season around Svalbard (Chang et al., 2011). If present, the continental factor is most likely of negligible abundance ~~for which reason~~ the PMF-analysis cannot differentiate it from other Oxygenated Organic Aerosol (OOA). Detailed information regarding the factor combination can be found in Supporting Information.

3 Results and Discussion

3.1 Time series

Time dependent OA, SO_4^{2-}, NO_3^-, NH_4^+, Cl and rBC concentrations [µg m^{-3}] measured by the SP-AMS are presented in Figure 1 together with temperature [°C], mean wind speed [m/s], and wind direction [°] for the time period 21 February to 23 May 2015. Weekly average concentrations ~~from the SP-AMS~~ can be found in Figure S6. Figure 1c shows the time dependent mass fraction of the different species. The total measured PM_1 concentration during the field study is relatively high, averaging 2.3 µg m^{-3}. It should be emphasized that this average does not consider particulate water, NaCl, and elements such as K, Ca, Si, Al and Fe. These elements may additionally contribute 0.1 – 0.2 µg/m^3 to PM_1 (Nguyen et al., 2013; Heidam et al., 2004). The measurement period covers the Arctic late winter and spring where high aerosol loadings are expected due to the favorable conditions for long-range transport of aerosols from mid-latitudes and slow particle removal rates. With regard to PM_1 concentration we hence observe the typical Arctic haze phenomenon. Generally, the area around VRS is dominated by winds from southwest (Nguyen et al., 2013), which is also evident during this campaign (Figure S1). As expected no diurnal pattern is observed for any of the chemical species indicating that the aerosols are regional and likely predominately from long-range transport.

During the entire campaign, SO_4^{2-} is the dominant species that on average makes up almost 70% of the PM_1 mass concentration ~~measured by the SP-AMS~~ (average 1.5 µg m^{-3}, Figure 1~~.~~b-c). This is in accordance with previous findings for SO_4^{2-} at VRS based on measurements with lower time-resolution (Nguyen et al., 2013; Fenger et al., 2013; Heidam et al., 2004). Atmospheric SO_4^{2-} is mainly formed as secondary inorganic ~~aerosols~~ and only a minor fraction is from primary emissions (Massling et al., 2015). Secondary SO_4^{2-} is ~~dominated by~~ atmospheric oxidation of sulfur dioxide (SO_2) and to a minor extent DMS (as the long-range transport is occurring over sea ice), and is dependent on the oxidative capacity of the atmosphere e.g. the concentration of hydroxyl radicals (OH). Secondary long-range transported SO_4^{2-} depends on atmospheric oxidation of SO_2 at its source regions, whereas local transformation (close

Atmos. Chem. Phys. Discuss., https://doi.org/10.5194/acp-2019-130
Manuscript under review for journal Atmos. Chem. Phys.
Discussion started: 25 March 2019

to VRS) of SO_2 leads to higher concentration of SO_4^{2-} from March, where solar radiation is sufficient with peak radiation exceeding 100 W/m^2 (Figure 3). This is consistent with results reported from other Arctic sites (Quinn et al., 2007; Gong et al., 2010; Heidam et al., 2004; Skov et al., 2017). Previous studies suggest that the main source of SO_2 and SO_4^{2-} at VRS is long-range transport of anthropogenic emissions mainly originating from Siberia (Heidam et al., 2004; Nguyen et al., 2013). In winter and early spring, direct emissions of sea-salt sulfate and photo-oxidation of oceanic emissions of DMS were expected to play a minor role since the ocean surrounding VRS is frozen at that time of the year (Heidam et al., 2004). From the beginning of April, the sea ice extent of the Northern Hemisphere is markedly reduced, and at the same time solar radiation increases (Figure 3). In this period, we observe MSA as an ion in the SP-AMS at *m/z* 78.9854. MSA is formed by atmospheric oxidation of DMS, which results from bacterial breakdown of dimethylsulfoniopropionate produced by marine phytoplankton and microalgae (Carpenter et al., 2012). DMS emerges steadily and peaks ~~in~~ the end of April (see Section 3.2). Oxidation of DMS may involve the hydroxyl radical, ozone, and halogen radicals such as Cl and BrO (Barnes et al., 2006; Hoffmann et al., 2016).

In this study, the OA fraction is the second largest contributor to PM$_1$ with an average concentration of 0.6 µg m^{-3}. Weekly averages showed a clear decrease from mid-April relative to the spring season concentrations (Figure 1). The OA time dependent concentration shows relatively large peaks during shorter time periods, which in some cases can be attributed to a change in wind direction from Southwesterly to Northerly winds (around 10°, Figure S1). While these wind directions were registered on a few occasions they potentially provided local pollution from the military station located three kilometers away from the measurement site. These peaks have not been discarded and the impacts of local pollution will be discussed further in Section 3.2.

Particulate NH_4^+ is found in much lower concentrations compared to OA and SO_4^{2-} with an average concentration of 0.09 µg m^{-3}. For the campaign, a significant correlation is found between SO_4^{2-} and NH_4^+. However, it is known that SO_4^{2-} and NH_4^+ do not originate from the same sources. SO_2, a key precursor to SO_4^{2-}, originates from combustion of fossil fuel and is oxidized to SO_4^{2-} in the atmosphere. In contrast, ammonia (NH_3) which is the precursor of NH_4^+, derives largely from long-range transport from farms and more locally from sea bird colonies (Croft et al., 2016). The strong correlation between SO_4^{2-} and NH_4^+ ($R^2 = 0.70$) suggests that the acidity of the particles is reasonably constant with time. This is furthermore in agreement with the general assumption that NH_4^+ is bound irreversibly to SO_4^{2-} (e.g. Seinfeld and Pandis, 1998), in this case as ammonium bisulfate. Particle~~-~~bound NH_4^+ has a much longer lifetime than NH_3 and therefore it is transported as NH_4^+ even to the high Arctic.

The average concentration of NO_3^- and Cl are 0.03 and 0.02 µg m^{-3}, respectively, which is close to the detection limits. These concentration levels are lower compared to what has previously been observed at VRS (Fenger et al., 2013; Heidam et al., 2004). However, the SP-AMS does not measure refractory ~~chlorine~~ species, such as NaCl. Moreover, Fenger et al. (2013) found that the overall size distribution of chloride and NO_3^- differed from SO_4^{2-}, with Cl and NO_3^- mainly found in supermicrometer particles (> 1 µm) not detectable by SP-AMS. These particles were suggested to originate from local/regional sources (frost flowers). Only during certain periods with specific wind directions NO_3^- and Cl were found in accumulation mode particles, which were ascribed to long-range transported particles (Fenger et al., 2013).

The average rBC concentration of 0.1 µg m^{-3} is above the lower detection limit (0.01 µg m^{-3}) and the highest rBC loadings are found in the first month of the campaign (February). As with OA, some of the spikes in the rBC time series are related to a change in wind direction and likely the result of local pollution from the military station. All data are included here and missing time periods of rBC (during April and May) are due to technical problems with the SP-AMS laser. BC is primarily emitted from both anthropogenic and natural combustion sources (Bond et al., 2013). Upon emission, aerosols containing BC grow by condensation and coagulation into the accumulation mode. Particles in the accumulation mode have the longest lifetime with respect to dry deposition and thus particles can be transported over longer distances during the Arctic haze period when precipitation is scarce (Bond et al., 2013; AMAP, 2011; Massling et al., 2015). These accumulation mode BC-containing particles may serve as cloud seeds in the late spring, when precipitation begins to be important in the Arctic (Garrett et al., 2011). Further, condensational growth of the BC-containing particles may increase the absorption by these particles (Cappa et al., 2012; Liu et al., 2015). Previous studies have found a correlation between BC and SO_4^{2-} at different Arctic stations (Massling et al., 2015; Eckhardt et al., 2015; Hirdman et al., 2010). These studies suggest that the two species are internally mixed and possibly undergo similar transport patterns. Furthermore, comparable correlation slopes were found for the different Arctic locations, which suggests that source regions of BC and SO_4^{2-} are similar for the entire Arctic. An even more recent study suggests that only a minor part of ambient aerosols contained rBC inclusions (Kodros et al., 2018). We also find a significant correlation between the two species (students t-test, level of significance 99.995), consistent with previous studies. However, we also find that the R^2 value is relatively low (0.18). The reason for this is that there are periods with particularly high rBC concentrations, likely originating from local emission sources (e.g. the military base), which will be investigated further in the following section. Additionally, in April and May SO_4^{2-} from DMS oxidation will make up a larger fraction of total SO_4^{2-}, and thereby reduce the ratio between rBC and SO_4^{2-}, which is also evident from Figure S4.

3.2 Source Apportionment

The PMF analysis was conducted for the HR OA mass spectra with one to five PMF factors and a three-factor solution was chosen (more details can be found in Supporting Information). Figure 2 shows the mass spectral profiles of the three different factors for the entire campaign period. Figure 3 illustrates time series for the factors and Table 2 shows the correlation of each factor with tracer species, respectively. Figure 4 illustrates the average mass concentration (µg m^{-3}) and the mass fraction of the factors in February, March, April and May. The PMF analysis yielded three factors: 1) a hydrocarbon-like organic aerosol factor (HOA), 2) an oxygenated Arctic haze organic aerosol factor (AOA) dominating winter and early spring, and 3) a more oxygenated marine organic aerosol factor (MOA) which builds up in late spring and becomes the dominating OA throughout late spring. The identification of these factors is discussed below.

The HOA factor is characterized by hydrocarbon fragments especially at *m/z* 41, 43, 55, 57, 67, 69 and 71 ($C_3H_5^+$, $C_3H_7^+$, $C_4H_7^+$, $C_4H_9^+$, $C_5H_7^+$, $C_5H_9^+$, $C_5H_{11}^+$, respectively) from chemically reduced organic emissions. The O/C ratio of 0.11, high signal at *m/z* 57 and the absence of CO_2^+ is a characteristic of primary combustion sources of fossil origin, which is similar to other HOA factors found in previous studies (Zhang et al., 2005; Aiken et al., 2009) and at other Arctic locations (Frossard et al., 2011). The very small contribution of the CO_2^+ ion at $m/z = 44$ and the very small abundances of typical biomass burning OA (BBOA) marker ions at *m/z* 60 ($C_2H_4O_2^+$) and *m/z* 73 ($C_3H_5O_2^+$) in the HOA factor spectrum suggests that the HOA factor is not mixed with BBOA. This finding is consistent with previous results that indicate BBOA levels are typically very low, based on measurements of levoglucosan in the Arctic, (Zangrando et al., 2013). The time series of HOA and rBC showed a moderate correlation ($R^2 = 0.35$), which is consistent with the HOA factor being of primary origin. The relatively low R^2 value (Table 2) can be partly explained by rBC being internally mixed with SO_4^{2-} and transported with the AOA factor. The HOA time series is generally higher in concentration at the beginning of the measurement period (Figure 4). The time series of HOA reveals a number of shorter periods with high mass loading, which could be caused by local pollution from the military station 2 km north of the measurement site due to a change in wind direction, or exhaust plumes from snow scooters and heavy-duty vehicles occasionally clearing the road nearby the measurement station for snow (see windrose, Figure S1). It is not trivial to distinguish local events and in this case the possible local contamination was investigated by comparing high HOA peaks (> 0.45 µg m^{-3}) with size distribution measurements from the SMPS (Lange et al., 2018). Periods which were attributed to local contamination accounted for less than 1% of OA concentration. Therefore, essentially the entire HOA concentration is assigned to long-range transportation, possibly sources with different ratios of HOA and rBC which would explain the moderate correlation between HOA and rBC.

The AOA is the most abundant factor from the beginning of the campaign through mid-April and accounts for 64% of OA mass for the entire field study (Figure 2b). The CO_2^+ ion contributes notably to the mass spectrum and the O:C is 0.63, indicating that this factor is likely secondary in origin. The dominating OA during the Arctic haze period is thus SOA, which results from long-range transport into the region during winter/spring. AOA is abundant during February to mid-April though lower concentrations are observed around middle of March. At the end of April and onwards the factor essentially disappears, which is in agreement with increasing wet deposition in the spring and a contracting polar dome impairing long-range transport into North Greenland (Abbatt et al., 2018). Generally, an OOA factor mainly consists of SOA but can also include oxygenated organic species from primary emissions (Zhang et al., 2005). In this case the AOA factor correlates significantly (level 99.995) with SO_4^{2-}, which is mainly formed by atmospheric oxidation of SO_2 suggesting the main part of the factor being SOA. The correlation is especially good until mid-April after which SO_4^{2-} beigns to correlate with MOA. The O/C ratio of 0.63 also indicates a less oxidized and fresher SOA factor, or an SOA formed from generally larger precursor VOCs, similar to what has been found in previous studies (O/C between 0.52 – 0.64, (Aiken et al., 2008~~)~~)). The AOA mass spectrum also included mass spectral peaks at *m/z* 60.021 ($C_2H_4O_2^+$) and 73.029 ($C_3H_5O_2$). These fragments are often taken as ~~being~~ indicative of

Atmos. Chem. Phys. Discuss., https://doi.org/10.5194/acp-2019-130
Manuscript under review for journal Atmos. Chem. Phys.
Discussion started: 25 March 2019

anhydrous sugar such as levoglucosan, and thereby suggest that biomass burning makes some contribution to Arctic OA. However, in this study biomass burning cannot be verified, since the abundance of $C_2H_4O_2^+$ did not exceed the expected contribution from SOA (Aiken et al., 2008; Aiken et al., 2009; Cubison et al., 2011; Lee et al., 2010; Saarnio et al., 2013). Biomass burning is generally assumed to play a significant role in the context of the composition of the Arctic aerosol (Stohl et al., 2013) where recent publication using isotopes of carbon reports biomass burning or biofuel use to account for up to 57% of EC at the Arctic station Zeppelin at Svalbard during high pollution events in winter (Winiger et al., 2015). However, levoglucosan is prone to atmospheric oxidation by hydroxide radicals (OH) (Hennigan et al., 2010; Hoffmann et al., 2010), which could degrade the markers during transport to North Greenland. This can explain the low abundance of levoglucosan markers measured in this study.

The MOA factor has a mass spectrum dominated by *m/z* 28 and 44 (CO^+ and CO_2^+), that is a more oxygenated OA factor due to the presence of e.g. organic acids and acid derived species, such as esters (Duplissy et al., 2011). A high O/C-ratio of 0.95 reveals that the factor is highly oxidized and photochemically aged. The MOA spectrum resembles a marine organic plume previously published from Mace Head, Ireland containing both primary and secondary organic aerosols of marine origin (Ovadnevaite et al., 2011). This spectrum and MOA in this study are different from the marine organic aerosol factor published during the ASCOS expedition in the Central Arctic Ocean (Chang et al., 2011), which shows a closer resemblance with the mass spectrum of pure MSA. In the MSA spectrum, *m/z* 15, 48, 64 and 79 are dominating peaks, which was also observed in the marine factor from the ASCOS expedition. The distinct peak at *m/z* 78.9854 is specific for MSA (Huang et al., 2017), and reveals that MOA has a secondary biogenic source (Becagli et al., 2013). The resemblance of MOA from this study with the mass spectrum from Mace Head indicates, that MOA is not solely a secondary marine source, but is most likely also composed by primary marine organic aerosols e.g. from sea spray (Ovadnevaite et al., 2011; Fu et al., 2015).

Figure 3 and 4 illustrate~~s~~ HOA and AOA decreasing around mid-April, while MOA builds up from the end of March. In 2015, Arctic sunrise ~~onset~~ at February 28th at VRS, where the sun became visible for a few minutes~~, only, above the mountains at the horizon~~. Polar daytime initiates photochemistry and hence the production of OH radicals (Seinfeld and Pandis, 2006) and reactive halogen radicals (Hoffmann et al., 2016; Barnes et al., 2006). From mid-April, the sun is above the horizon all day until the beginning of September. Still solar radiation varies over the day and hence the OH production. In contrast, the concentration of OH during build up of Arctic haze is correspondingly low with ozone being the major oxidant during the dark winter. In Figure 3, the daily averaged solar radiation (W m^{-2}) and sea ice extent (km^2) ~~o~~n the ~~Northern Hemisphere~~ are shown together with the time series of MOA. While MOA is less abundant during February and March, this factor greatly increases in April, when radiation exceeds approximately 100 W m^{-2}. In April, the highest OA concentrations is observed where AOA accounts for around 70% of OA (Figure 4). In May, MOA becomes the dominating OA while AOA nearly disappears. At the same time we observe the lowest concentration of OA consisting of 75% MOA (Figure 4). This is significantly higher than observed at Alert (Narukawa et al., 2008). Until the beginning of April, the sea ice extent is constant at around 14.5 million km^2 ~~on the Northern Hemisphere~~ (Figure 3). Hereafter, about a month after the onset of polar daytime, the sea ice surface area starts to decline. After 6 weeks starting from a constant sea-ice extent in mid-May, it is reduced by 2 million km^2 corresponding to a 14% loss of ice-covered surface area. Consequently, more open waters allow for higher DMS emissions and atmospheric oxidation of DMS to MSA involving OH. Also open leads and marginal ice zones provide primary marine aerosols (Willis et al., 2018). Indeed, previous findings suggest that biogenic productivity in open oceans and sea ice zones and the emission of DMS are responsible for increased new particle formation, as sea ice pack extent retreats (Dall'Osto et al., 2017). Quinn and co-workers reported increased concentrations of MSA at Barrow from 2000 to 2009 associated with the northward migration of the marginal ice zone (Quinn et al., 2009; Sharma et al., 2012; Laing et al., 2013). Of the four northernmost year-round manned observatories at Alert, Mount Zeppelin, VRS and Barrow, the highest MSA concentrations are measured at Mount Zeppelin, likely due to its proximity to open waters around Svalbard, which are a significant source of DMS from May to August (e.g. Lana et al. ~~(~~2011~~)~~)). This contrasts with the ice situation around VRS, ~~which is~~ ice covered most of the year.

Considering the stronger oxidizing environment starting in April, we expect MOA to be abundant until autumn, and possibly co-exist with an emerging continental factor as reported during the ASCOS cruise track in late summer/autumn (Chang et al., 2011). MOA constitutes only 22% of OA on average during our measurement period. However, the radiative impact may be greater than the other OA types because it emerged after polar sunrise and persisted during polar daytime for which reason they are optically active 24 hours a day although solar radiation has a diurnal cycle. Moreover, MOA is by far the most abundant OA from end of April and onwards. The observed transition between AOA and MOA is in agreement with Narukawa et al. (2008), who observed a transition between fossil fuel influenced OA to marine OA. MOA is not only secondary but may contain oxidation products of DMS and other VOCs from oceanic origin, and primary components including colloidal gels (Croft et al., 2018; Leck and Bigg, 2005; Orellana et al., 2011). In line with our findings, modelling at several sites in the Canadian Arctic suggested that marine OA may account for more than half of the summertime OA (Croft et al., 2018). Biogenic marine aerosols can scatter solar radiation, which will result in a negative radiative forcing. Biogenic marine aerosols can also coat soot particles, which may be transported from wild fires (AMAP, 2015), which could impact the CCN activity and absorption by the soot particles, with the latter potentially enhancing the warming influence of the particles (Lange et al., 2018). These findings encourage further studies of optical properties and chemical composition and physico-chemical parameters as CCN ability or hygroscopicity of aerosols prevailing during polar daytime.

4 Conclusion

In the transition from polar night to polar day we concluded SO_4^{2-} to be the most abundant species in submicrometer aerosols averaging 1.5 µg m^{-3} during February to May 2015 and decreasing throughout the campaign period. This is in accordance with previous findings from VRS and Svalbard (Udisti et al., 2016) where SO_4^{2-} has been apportioned to be 75% anthropogenic, while natural contributions from crustal, sea salt and biogenic sources contributed minorly by 3%, 12% and 2%. While not previously quantified at VRS, OA was found to contribute 22% of measured PM_1. Based on the SP-AMS measurements the submicrometer aerosol mass concentration averaged 2.3 µg m^{-3} during the campaign period. Organic species and SO_4^{2-} have the potential to condense on and coat black carbon, which averaged 0.1 µg m^{-3}, potentially impacting the CCN activity of and light absorption by BC. However, the chemical composition should be further studied in summer and autumn.

The OA was overall highly oxidized. Source apportionment analysis yielded three factors, identified as a Hydrocarbon-like Organic Aerosol (HOA), Arctic haze Organic Aerosol (AOA) and Marine Organic Aerosol (MOA) with O/C ratios of 0.11, 0.63 and 0.95, respectively. HOA, being the most reduced factor, made up 12% of OA of which 1 % of OA was demonstrated to be contamination from the nearby military camp. AOA and MOA made up 86% of OA averaged across the campaign, with AOA averaging 64% and MOA 22% (2% residuals). AOA was most likely secondary while MOA contained both MSA (secondary OA) and a mass spectrum indicating the presence of primary OA as well. The sum of long-range transported HOA and AOA make-up the vast majority of OA during the Arctic haze period. AOA and MOA exhibit distinct temporal variability. The less oxidized AOA builds up during the Arctic haze period and dominates until early spring, during which both the absolute and relative contribution to the OA burden decreases substantially. In contrast, the MOA is nearly non-existant until early spring but is then by far the dominating OA from the end of April and onwards. The fact that MOA emerges at a time where long-range transport is impaired by increased deposition and a contracting polar dome indicates that the sources to this factor are more Arctic regional in nature. This demonstrates the importance of biogenic sources in the Arctic, especially in the spring. In view of changing biogenic processes and corresponding source strengths of aerosol precursors in a changing Arctic climate with changing sea-ice extent, additional high time resolution measurements are urgently needed in order to elucidate the organic components dominating aerosol summer mass and number concentrations.

Supporting information

Supporting information describes site information, supplementary instruments, collection efficiency, validation of SP-AMS data, and key diagnostics for the PMF solution.

Author contribution

Ingeborg E. Nielsen and Jacob K. Nøjgaard carried out the field measurements, and Ingeborg did the analysis of the SP-AMS data. Jacob and Ingeborg carried out the PMF analysis and took lead in writing the manuscript. Henrik Skov supervised the project and provided critical feedback, he participated in the fieldcampaign and helped shape the research and manuscript. Heikki Junninen and Nina Sarnela helped monitor the SP-AMS during the field campaign and commented on the manuscript. Sonya Collier, Qi Zhang and Christopher D. Cappa helped interpret the SP-AMS data set and provided critical feedback on the manuscript. Andreas Massling and Robert Lange participated in the fieldcampaign and discussed the analysis and commented on the manuscript. Axel C. Eriksson and Manuel Dall'Osto discussed the analysis and results and commented on the manuscript.

Acknowledgements

The research was financially supported by the Arctic Centre of Research at Aarhus University, Cryosphere-Atmosphere Interaction in a Changing Arctic Climate (CRAICC), WOOD combustion - detailed Monitoring related to Acute effects in Denmark (WOODMAD), the Danish Environmental Protection Agency with means from the MIKA/DANCEA funds for environmental support to the Arctic Region and the Danish Council for Independent Research (project NUMEN, DFF-FTP-4005-00485B). Special thanks go to laboratory technician Bjarne Jensen and the staff at Station Nord for great support during the field campaign. Sissel Bjørn Svendsen is greatly acknowledged for her data control of the SMPS data and the Villum Foundation is acknowledged for financing the new research station, Villum Research Station, at Station Nord.

References

Abbatt, J. P. D., Leaitch, W. R., Aliabadi, A. A., Bertram, A. K., Blanchet, J. P., Boivin-Rioux, A., Bozem, H., Burkart, J., Chang, R. Y. W., Charette, J., Chaubey, J. P., Christensen, R. J., Cirisan, A., Collins, D. B., Croft, B., Dionne, J., Evans, G. J., Fletcher, C. G., Ghahremaninezhad, R., Girard, E., Gong, W., Gosselin, M., Gourdal, M., Hanna, S. J., Hayashida, H., Herber, A. B., Hesaraki, S., Hoor, P., Huang, L., Hussherr, R., Irish, V. E., Keita, S. A., Kodros, J. K., Köllner, F., Kolonjari, F., Kunkel, D., Ladino, L. A., Law, K., Levasseur, M., Libois, Q., Liggio, J., Lizotte, M., Macdonald, K. M., Mahmood, R., Martin, R. V., Mason, R. H., Miller, L. A., Moravek, A., Mortenson, E., Mungall, E. L., Murphy, J. G., Namazi, M., Norman, A. L., O'Neill, N. T., Pierce, J. R., Russell, L. M., Schneider, J., Schulz, H., Sharma, S., Si, M., Staebler, R. M., Steiner, N. S., Galí, M., Thomas, J. L., von Salzen, K., Wentzell, J. J. B., Willis, M. D., Wentworth, G. R., Xu, J. W., and Yakobi-Hancock, J. D.: New insights into aerosol and climate in the Arctic, Atmos. Chem. Phys. Discuss., 2018, 1-60, https://doi.org/10.5194/acp-2018-995, in review, 2018.

Aiken, A. C., Decarlo, P. F., Kroll, J. H., Worsnop, D. R., Huffman, J. A., Docherty, K. S., Ulbrich, I. M., Mohr, C., Kimmel, J. R., Sueper, D., Sun, Y., Zhang, Q., Trimborn, A., Northway, M., Ziemann, P. J., Canagaratna, M. R., Onasch, T. B., Alfarra, M. R., Prevot, A. S. H., Dommen, J., Duplissy, J., Metzger, A., Baltensperger, U., and Jimenez, J. L.: O/C and OM/OC ratios of primary, secondary, and ambient organic aerosols with high-resolution time-of-flight aerosol mass spectrometry, Environ. Sci. Technol., 42, 4478-4485, https://doi.org/10.1021/es703009q, 2008.

Aiken, A. C., Salcedo, D., Cubison, M. J., Huffman, J. A., DeCarlo, P. F., Ulbrich, I. M., Docherty, K. S., Sueper, D., Kimmel, J. R., Worsnop, D. R., Trimborn, A., Northway, M., Stone, E. A., Schauer, J. J., Volkamer, R. M., Fortner, E., de Foy, B., Wang, J., Laskin, A., Shutthanandan, V., Zheng, J., Zhang, R., Gaffney, J., Marley, N. A., Paredes-Miranda, G., Arnott, W. P., Molina, L. T., Sosa, G., and Jimenez, J. L.: Mexico City aerosol analysis during MILAGRO using high resolution aerosol mass spectrometry at the urban supersite (T0) - Part 1: Fine particle composition and organic source apportionment, Atmos. Chem. Phys., 9, 6633-6653, https://doi.org/10.5194/acp-9-6633-2009, 2009.

Allan, J. D., Jimenez, J. L., Williams, P. I., Alfarra, M. R., Bower, K. N., Jayne, J. T., Coe, H., and Worsnop, D. R.: Quantitative sampling using an Aerodyne aerosol mass spectrometer: 1. Techniques of data interpretation and error analysis, J. Geophys. Res.: Atmos., 108, Artn 4283, https://doi.org/10.1029/2003jd001607, 2003.

Allan, J. D., Delia, A. E., Coe, H., Bower, K. N., Alfarra, M. R., Jimenez, J. L., Middlebrook, A. M., Drewnick, F., Onasch, T. B., Canagaratna, M. R., Jayne, J. T., and Worsnop, D. R.: A generalised method for the extraction of chemically resolved mass spectra from Aerodyne aerosol mass spectrometer data, J. Aerosol Sci., 35, 909-922, https://doi.org/10.1016/j.jaerosci.2004.02.007, 2004.

AMAP: The Impact of Black Carbon on Arctic Climate (2011). By: P.K. Quinn, A. Stohl, A. Arneth, T. Berntsen, J. F. Burkhart, J. Christensen, M. Flanner, K. Kupiainen, H. Lihavainen, M. Shepherd, V. Shevchenko, H. Skov, and V. Vestreng. AMAP Technical Report No. 4 (2011). Arctic Monitoring and Assessment Programme (AMAP), Oslo, 72 pp., 2011.

AMAP: AMAP Assessment 2015: Black carbon and ozone as Arctic climate forcers, Arctic Monitoring and Assessment Programme (AMAP), Oslo, Norway, vii + 166 pp., 2015.

AMAP: Snow, Water, Ice and Permafrost in the Arctic (SWIPA) 2017, Arctic Monitoring and Assessment Programme (AMAP), Oslo, Norway, xiv + 269 pp., 2017.

Andrews, E., Ogren, J. A., Bonasoni, P., Marinoni, A., Cuevas, E., Rodriguez, S., Sun, J. Y., Jaffe, D. A., Fischer, E. V., Baltensperger, U., Weingartner, E., Coen, M. C., Sharma, S., Macdonald, A. M., Leaitch, W. R., Lin, N. H., Laj, P., Arsov, T., Kalapov, I., Jefferson, A., and Sheridan, P.: Climatology of aerosol radiative properties in the free troposphere, Atmos. Res., 102, 365-393, https://doi.org/10.1016/j.atmosres.2011.08.017, 2011.

Barnes, I., Hjorth, J., and Mihalopoulos, N.: Dimethyl sulfide and dimethyl sulfoxide and their oxidation in the atmosphere, Chem. Rev., 106, 940-975, https://doi.org/10.1021/cr020529+, 2006.

Barrett, T. E., Robinson, E. M., Usenko, S., and Sheesley, R. J.: Source Contributions to Wintertime Elemental and Organic Carbon in the Western Arctic Based on Radiocarbon and Tracer Apportionment, Environ. Sci. Technol., 49, 13733-13733, https://doi.org/10.1021/acs.est.5b05128, 2015.

Barrie, L. A., Hoff, R. M., and Daggupaty, S. M.: The Influence of Mid-Latitudinal Pollution Sources on Haze in the Canadian Arctic, Atmos. Environ., 15, 1407-1419, https://doi.org/10.1016/0004-6981(81)90347-4, 1981.

Becagli, S., Lazzara, L., Fani, F., Marchese, C., Traversi, R., Severi, M., di Sarra, A., Sferlazzo, D., Piacentino, S., Bommarito, C., Dayan, U., and Udisti, R.: Relationship between methanesulfonate (MS-) in atmospheric particulate and remotely sensed phytoplankton activity in oligo-mesotrophic central

Mediterranean Sea, Atmos. Environ., 79, 681-688, https://doi.org/10.1016/j.atmosenv.2013.07.032, 2013.

Bond, T. C., Doherty, S. J., Fahey, D. W., Forster, P. M., Berntsen, T., DeAngelo, B. J., Flanner, M. G., Ghan, S., Karcher, B., Koch, D., Kinne, S., Kondo, Y., Quinn, P. K., Sarofim, M. C., Schultz, M. G., Schulz, M., Venkataraman, C., Zhang, H., Zhang, S., Bellouin, N., Guttikunda, S. K., Hopke, P. K., Jacobson, M. Z., Kaiser, J. W., Klimont, Z., Lohmann, U., Schwarz, J. P., Shindell, D., Storelvmo, T., Warren, S. G., and Zender, C. S.: Bounding the role of black carbon in the climate system: A scientific assessment, J. Geophys. Res.: Atmos., 118, 5380-5552, https://doi.org/10.1002/jgrd.50171, 2013.

Brock, C. A., Cozic, J., Bahreini, R., Froyd, K. D., Middlebrook, A. M., McComiskey, A., Brioude, J., Cooper, O. R., Stohl, A., Aikin, K. C., de Gouw, J. A., Fahey, D. W., Ferrare, R. A., Gao, R. S., Gore, W., Holloway, J. S., Hubler, G., Jefferson, A., Lack, D. A., Lance, S., Moore, R. H., Murphy, D. M., Nenes, A., Novelli, P. C., Nowak, J. B., Ogren, J. A., Peischl, J., Pierce, R. B., Pilewskie, P., Quinn, P. K., Ryerson, T. B., Schmidt, K. S., Schwarz, J. P., Sodemann, H., Spackman, J. R., Stark, H., Thomson, D. S., Thornberry, T., Veres, P., Watts, L. A., Warneke, C., and Wollny, A. G.: Characteristics, sources, and transport of aerosols measured in spring 2008 during the aerosol, radiation, and cloud processes affecting Arctic Climate (ARCPAC) Project, Atmos. Chem. Phys., 11, 2423-2453, https://doi.org/10.5194/acp-11-2423-2011, 2011.

Canagaratna, M. R., Jayne, J. T., Jimenez, J. L., Allan, J. D., Alfarra, M. R., Zhang, Q., Onasch, T. B., Drewnick, F., Coe, H., Middlebrook, A., Delia, A., Williams, L. R., Trimborn, A. M., Northway, M. J., DeCarlo, P. F., Kolb, C. E., Davidovits, P., and Worsnop, D. R.: Chemical and microphysical characterization of ambient aerosols with the aerodyne aerosol mass spectrometer, Mass Spectrom. Rev., 26, 185-222, https://doi.org/10.1002/mas.20115, 2007.

Cappa, C. D., Onasch, T. B., Massoli, P., Worsnop, D. R., Bates, T. S., Cross, E. S., Davidovits, P., Hakala, J., Hayden, K. L., Jobson, B. T., Kolesar, K. R., Lack, D. A., Lerner, B. M., Li, S.-M., Mellon, D., Nuaaman, I., Olfert, J. S., Petäjä, T., Quinn, P. K., Song, C., Subramanian, R., Williams, E. J., and Zaveri, R. A.: Radiative absorption enhancements due to the mixing state of atmospheric black carbon, Science, 337, 1078-1081, https://doi.org/10.1126/science.1223447, 2012.

Carpenter, L. J., Archer, S. D., and Beale, R.: Ocean-atmosphere trace gas exchange, Chem. Soc. Rev., 41, 6473-6506, https://doi.org/10.1039/c2cs35121h, 2012.

Chang, R. Y. W., Leck, C., Graus, M., Muller, M., Paatero, J., Burkhart, J. F., Stohl, A., Orr, L. H., Hayden, K., Li, S. M., Hansel, A., Tjernstrom, M., Leaitch, W. R., and Abbatt, J. P. D.: Aerosol composition and sources in the central Arctic Ocean during ASCOS, Atmos. Chem. Phys., 11, 10619-10636, https://doi.org/10.5194/acp-11-10619-2011, 2011.

Christensen, J. H.: The Danish eulerian hemispheric model — a three-dimensional air pollution model used for the arctic, Atmos. Environ., 31, 4169-4191, https://doi.org/10.1016/s1352-2310(97)00264-1, 1997.

Croft, B., Wentworth, G. R., Martin, R. V., Leaitch, W. R., Murphy, J. G., Murphy, B. N., Kodros, J. K., Abbatt, J. P. D., and Pierce, J. R.: Contribution of Arctic seabird-colony ammonia to atmospheric particles and cloud-albedo radiative effect, Nat. Commun., 7, Artn 13444, https://doi.org/10.1038/ncomms13444, 2016.

Croft, B., Martin, R. V., Leaitch, W. R., Burkart, J., Chang, R. Y. W., Collins, D. B., Hayes, P. L., Hodshire, A. L., Huang, L., Kodros, J. K., Moravek, A., Mungall, E. L., Murphy, J. G., Sharma, S., Tremblay, S., Wentworth, G. R., Willis, M. D., Abbatt, J. P. D., and Pierce, R. P.: Arctic marine secondary organic aerosol contributes significantly to summertime particle size distributions in the Canadian Arctic Archipelago, Atmos. Chem. Phys. Discuss., https://doi.org/doi.org/10.5194/acp-2018-895, in review, 2018.

Cubison, M. J., Ortega, A. M., Hayes, P. L., Farmer, D. K., Day, D., Lechner, M. J., Brune, W. H., Apel, E., Diskin, G. S., Fisher, J. A., Fuelberg, H. E., Hecobian, A., Knapp, D. J., Mikoviny, T., Riemer, D., Sachse, G. W., Sessions, W., Weber, R. J., Weinheimer, A. J., Wisthaler, A., and Jimenez, J. L.: Effects of aging on organic aerosol from open biomass burning smoke in aircraft and laboratory studies, Atmos. Chem. Phys., 11, 12049-12064, https://doi.org/10.5194/acp-11-12049-2011, 2011.

Dall'Osto, M., Beddows, D. C. S., Tunved, P., Krejci, R., Strom, J., Hansson, H. C., Yoon, Y. J., Park, K. T., Becagli, S., Udisti, R., Onasch, T., O'Dowd, C. D., Simo, R., and Harrison, R. M.: Arctic sea ice melt leads to atmospheric new particle formation, Sci Rep-Uk, 7, ARTN 3318, https://doi.org/10.1038/s41598-017-03328-1, 2017.

DeCarlo, P. F., Kimmel, J. R., Trimborn, A., Northway, M. J., Jayne, J. T., Aiken, A. C., Gonin, M., Fuhrer, K., Horvath, T., Docherty, K. S., Worsnop, D. R., and Jimenez, J. L.: Field-deployable, high-resolution, time-of-flight aerosol mass spectrometer, Anal. Chem., 78, 8281-8289, https://doi.org/10.1021/ac061249n, 2006.

Dillner, A. M., Phuah, C. H., and Turner, J. R.: Effects of post-sampling conditions on ambient carbon aerosol filter measurements, Atmos. Environ., 43, 5937-5943, https://doi.org/10.1016/j.atmosenv.2009.08.009, 2009.

Drewnick, F., Hings, S. S., DeCarlo, P., Jayne, J. T., Gonin, M., Fuhrer, K., Weimer, S., Jimenez, J. L., Demerjian, K. L., Borrmann, S., and Worsnop, D. R.: A new time-of-flight aerosol mass spectrometer (TOF-AMS) - Instrument description and first field deployment, Aerosol Sci. Technol., 39, 637-658, https://doi.org/10.1080/02786820500182040, 2005.

Duplissy, J., DeCarlo, P. F., Dommen, J., Alfarra, M. R., Metzger, A., Barmpadimos, I., Prevot, A. S. H., Weingartner, E., Tritscher, T., Gysel, M., Aiken, A. C., Jimenez, J. L., Canagaratna, M. R., Worsnop, D. R., Collins, D. R., Tomlinson, J., and Baltensperger, U.: Relating hygroscopicity and composition of organic aerosol particulate matter, Atmos. Chem. Phys., 11, 1155-1165, https://doi.org/10.5194/acp-11-1155-2011, 2011.

Earle, M. E., Liu, P. S. K., Strapp, J. W., Zelenyuk, A., Imre, D., McFarquhar, G. M., Shantz, N. C., and Leaitch, W. R.: Factors influencing the microphysics and radiative properties of liquid-dominated Arctic clouds: Insight from observations of aerosol and clouds during ISDAC, J. Geophys. Res.: Atmos., 116, Artn D00t09, https://doi.org/10.1029/2011jd015887, 2011.

Eckhardt, S., Quennehen, B., Olivie, D. J. L., Berntsen, T. K., Cherian, R., Christensen, J. H., Collins, W., Crepinsek, S., Daskalakis, N., Flanner, M., Herber, A., Heyes, C., Hodnebrog, O., Huang, L., Kanakidou, M., Klimont, Z., Langner, J., Law, K. S., Lund, M. T., Mahmood, R., Massling, A., Myriokefalitakis, S., Nielsen, I. E., Nojgaard, J. K., Quaas, J., Quinn, P. K., Raut, J. C., Rumbold, S. T., Schulz, M., Sharma, S., Skeie, R. B., Skov, H., Uttal, T., von Salzen, K., and Stohl, A.: Current model capabilities for simulating black carbon and sulfate concentrations in the Arctic atmosphere: a multi-model evaluation using a comprehensive measurement data set, Atmos. Chem. Phys., 15, 9413-9433, https://doi.org/10.5194/acp-15-9413-2015, 2015.

Fenger, M., Sørensen, L. L., Kristensen, K., Jensen, B., Nguyen, Q. T., Nøjgaard, J. K., Massling, A., Skov, H., Becker, T., and Glasius, M.: Sources of anions in aerosols in northeast Greenland during late winter, Atmos. Chem. Phys., 13, 1569-1578, https://doi.org/10.5194/acp-13-1569-2013, 2013.

Frossard, A. A., Shaw, P. M., Russell, L. M., Kroll, J. H., Canagaratna, M. R., Worsnop, D. R., Quinn, P. K., and Bates, T. S.: Springtime Arctic haze contributions of submicron organic particles from European and Asian combustion sources, J. Geophys. Res.: Atmos., 116, Artn D05205, https://doi.org/10.1029/2010jd015178, 2011.

Fu, P. Q., Kawamura, K., Chen, J., Qin, M. Y., Ren, L. J., Sun, Y. L., Wang, Z. F., Barrie, L. A., Tachibana, E., Ding, A. J., and Yamashita, Y.: Fluorescent water-soluble organic aerosols in the High Arctic atmosphere, Sci Rep-Uk, 5, ARTN 9845, https://doi.org/10.1038/srep09845, 2015.

Garrett, T. J., Brattstrom, S., Sharma, S., Worthy, D. E. J., and Novelli, P.: The role of scavenging in the seasonal transport of black carbon and sulfate to the Arctic, Geophys. Res. Lett., 38, https://doi.org/10.1029/2011GL048221, 2011.

Gong, S. L., Zhao, T. L., Sharma, S., Toom-Sauntry, D., Lavoue, D., Zhang, X. B., Leaitch, W. R., and Barrie, L. A.: Identification of trends and interannual variability of sulfate and black carbon in the Canadian High Arctic: 1981-2007, J. Geophys. Res.: Atmos., 115, Artn D07305, https://doi.org/10.1029/2009jd012943, 2010.

Heidam, N. Z.: The Components of the Arctic Aerosol, Atmos. Environ., 18, 329-343, https://doi.org/10.1016/0004-6981(84)90107-0, 1984.

Heidam, N. Z., Wahlin, P., and Christensen, J. H.: Tropospheric gases and aerosols in Northeast Greenland, Journal of the Atmospheric Sciences, 56, 261-278, https://doi.org/10.1175/1520-0469(1999)056<0261:tgaain>2.0.co;2, 1999.

Heidam, N. Z., Christensen, J., Wåhlin, P., and Skov, H.: Arctic atmospheric contaminants in NE Greenland: levels, variations, origins, transport, transformations and trends 1990-2001, Sci. Total Environ., 331, 5-28, https://doi.org/10.1016/j.scitotenv.2004.03.033, 2004.

Hennigan, C. J., Sullivan, A. P., Collett, J. L., and Robinson, A. L.: Levoglucosan stability in biomass burning particles exposed to hydroxyl radicals, Geophys. Res. Lett., 37, L09806, https://doi.org/10.1029/2010gl043088, 2010.

Hirdman, D., Burkhart, J. F., Sodemann, H., Eckhardt, S., Jefferson, A., Quinn, P. K., Sharma, S., Strom, J., and Stohl, A.: Long-term trends of black carbon and sulphate aerosol in the Arctic: changes in atmospheric transport and source region emissions, Atmos. Chem. Phys., 10, 9351-9368, https://doi.org/10.5194/acp-10-9351-2010, 2010.

Hoffmann, D., Tilgner, A., Iinuma, Y., and Herrmann, H.: Atmospheric Stability of Levoglucosan: A Detailed Laboratory and Modeling Study, Environ. Sci. Technol., 44, 694-699, https://doi.org/10.1021/es902476f, 2010.

Hoffmann, E. H., Tilgner, A., Schrodner, R., Brauera, P., Wolke, R., and Herrmann, H.: An advanced modeling study on the impacts and atmospheric implications of multiphase dimethyl sulfide chemistry, Proceedings of the National Academy of Sciences of the United States of America, 113, 11776-11781, https://doi.org/10.1073/pnas.1606320113, 2016.

Huang, S., Poulain, L., van Pinxteren, D., van Pinxteren, M., Wu, Z. J., Herrmann, H., and Wiedensohler, A.: Latitudinal and Seasonal Distribution of Particulate MSA over the Atlantic using a Validated Quantification Method with HR-ToF-AMS, Environ. Sci. Technol., 51, 418-426, https://doi.org/10.1021/acs.est.6b03186, 2017.

IPCC: Climate Change 2013: The Physical Science Basis. Contribution of Working Group I to the Fifth Assessment Report of the Intergovernmental Panel on Climate Change, Cambridge University Press, Cambridge, United Kingdom and New York, NY, USA, 1535 pp., 2013.

Jayne, J. T., Leard, D. C., Zhang, X., Davidovits, P., Smith, K. A., Kolb, C. E., and Worsnop, D. R.: Development of an Aerosol Mass Spectrometer for Size and Composition Analysis of Submicron Particles, Aerosol Sci. Technol., 33, 49-70, https://doi.org/10.1080/027868200410840, 2000.

Jimenez, J. L., Jayne, J. T., Shi, Q., Kolb, C. E., Worsnop, D. R., Yourshaw, I., Seinfeld, J. H., Flagan, R. C., Zhang, X. F., Smith, K. A., Morris, J. W., and Davidovits, P.: Ambient aerosol sampling using the Aerodyne Aerosol Mass Spectrometer, J. Geophys. Res.: Atmos., 108, Artn 8425, https://doi.org/10.1029/2001jd001213, 2003.

Kawamura, K., Kasukabe, H., and Barrie, L. A.: Secondary formation of water-soluble organic acids and alpha-dicarbonyls and their contributions to total carbon and water-soluble organic carbon: Photochemical aging of organic aerosols in the Arctic spring, J. Geophys. Res.: Atmos., 115, Artn D21306, https://doi.org/10.1029/2010jd014299, 2010.

Kodros, J. K., Hanna, S. J., Bertram, A. K., Leaitch, W. R., Schulz, H., Herber, A. B., Zanatta, M., Burkart, J., Willis, M. D., Abbatt, J. P. D., and Pierce, J. R.: Size-resolved mixing state of black carbon in the Canadian high Arctic and implications for simulated direct radiative effect, Atmos. Chem. Phys., 18, 11345-11361, https://doi.org/10.5194/acp-18-11345-2018, 2018.

Komppula, M., Lihavainen, H., Kerminen, V. M., Kulmala, M., and Viisanen, Y.: Measurements of cloud droplet activation of aerosol particles at a clean subarctic background site, J. Geophys. Res.: Atmos., 110, Artn D06204, https://doi.org/10.1029/2004jd005200, 2005.

Laing, J. R., Hopke, P. K., Hopke, E. F., Husain, L., Dutkiewicz, V. A., Paatero, J., and Viisanen, Y.: Long-term trends of biogenic sulfur aerosol and its relationship with sea surface temperature in Arctic Finland, J. Geophys. Res.: Atmos., 118, Artn 776, 11770-11776, https://doi.org/10.1002/2013jd020384, 2013.

Lana, A., Bell, T. G., Simo, R., Vallina, S. M., Ballabrera-Poy, J., Kettle, A. J., Dachs, J., Bopp, L., Saltzman, E. S., Stefels, J., Johnson, J. E., and Liss, P. S.: An updated climatology of surface dimethlysulfide concentrations and emission fluxes in the global ocean, Global Biogeochem. Cycles, 25, Artn Gb1004, https://doi.org/10.1029/2010gb003850, 2011.

Lange, R., Dall'Osto, M., Skov, H., Nojgaard, J. K., Nielsen, I. E., Beddowse, D. C. S., Simob, R., Harrison, R. M., and Massling, A.: Characterization of distinct Arctic aerosol accumulation modes and their sources, Atmos. Environ., 183, 1-10, https://doi.org/10.1016/j.atmosenv.2018.03.060, 2018.

Lanz, V. A., Alfarra, M. R., Baltensperger, U., Buchmann, B., Hueglin, C., and Prevot, A. S. H.: Source apportionment of submicron organic aerosols at an urban site by factor analytical modelling of aerosol mass spectra, Atmos. Chem. Phys., 7, 1503-1522, https://doi.org/10.5194/acp-7-1503-2007, 2007.

Law, K. S., and Stohl, A.: Arctic Air Pollution: Origins and Impacts, Science, 315, 1537-1540, https://doi.org/10.1126/science.1137695, 2007.

Leaitch, W. R., Russell, L. M., Liu, J., Kolonjari, F., Toom, D., Huang, L., Sharma, S., Chivulescu, A., Veber, D., and Zhang, W. D.: Organic functional groups in the submicron aerosol at 82.5 degrees N, 62.5

degrees W from 2012 to 2014, Atmos. Chem. Phys., 18, 3269-3287, https://doi.org/10.5194/acp-18-3269-2018, 2018.

Leck, C., and Bigg, E. K.: Source and evolution of the marine aerosol - A new perspective, Geophys. Res. Lett., 32, Artn L19803, https://doi.org/10.1029/2005gl023651, 2005.

Lee, B. P., Li, Y. J., Yu, J. Z., Louie, P. K. K., and Chan, C. K.: Physical and chemical characterization of ambient aerosol by HR-ToF-AMS at a suburban site in Hong Kong during springtime 2011, J. Geophys. Res.: Atmos., 118, 8625-8639, https://doi.org/10.1002/jgrd.50658, 2013.

Lee, T., Sullivan, A. P., Mack, L., Jimenez, J. L., Kreidenweis, S. M., Onasch, T. B., Worsnop, D. R., Malm, W., Wold, C. E., Hao, W. M., and Collett, J. L.: Chemical Smoke Marker Emissions During Flaming and Smoldering Phases of Laboratory Open Burning of Wildland Fuels, Aerosol Sci. Technol., 44, I-V, https://doi.org/10.1080/02786826.2010.499884, 2010.

Lenton, T. M.: Arctic climate tipping points, A Journal of the Human Environment, 41, 10-22, https://doi.org/10.1007/s13280-011-0221-x, 2012.

Liu, S., Aiken, A. C., Gorkowski, K., Dubey, M. K., Cappa, C. D., Williams, L. R., Herndon, S. C., Massoli, P., Fortner, E. C., Chhabra, P. S., Brooks, W. A., Onasch, T. B., Jayne, J. T., Worsnop, D. R., China, S., Sharma, N., Mazzoleni, C., Xu, L., Ng, N. L., Liu, D., Allan, J. D., Lee, J. D., Fleming, Z. L., Mohr, C., Zotter, P., Szidat, S., and Prevot, A. S. H.: Enhanced light absorption by mixed source black and brown carbon particles in UK winter, Nat. Commun., 6, No. 8435, https://doi.org/10.1038/ncomms9435, 2015.

Mahmood, R., von Salzen, K., Flanner, M., Sand, M., Langner, J., Wang, H. L., and Huang, L.: Seasonality of global and Arctic black carbon processes in the Arctic Monitoring and Assessment Programme models, J. Geophys. Res.: Atmos., 121, 7100-7116, https://doi.org/10.1002/2016jd024849, 2016.

Martinsson, J., Eriksson, A. C., Nielsen, I. E., Malmborg, V. B., Ahlberg, E., Andersen, C., Lindgren, R., Nystrom, R., Nordin, E. Z., Brune, W. H., Svenningsson, B., Swietlicki, E., Boman, C., and Pagels, J. H.: Impacts of Combustion Conditions and Photochemical Processing on the Light Absorption of Biomass Combustion Aerosol, Environ. Sci. Technol., 49, 14663-14671, https://doi.org/10.1021/acs.est.5b03205, 2015.

Massling, A., Nielsen, I. E., Kristensen, D., Christensen, J. H., Sorensen, L. L., Jensen, B., Nguyen, Q. T., Nojgaard, J. K., Glasius, M., and Skov, H.: Atmospheric black carbon and sulfate concentrations in Northeast Greenland, Atmos. Chem. Phys., 15, 9681-9692, https://doi.org/10.5194/acp-15-9681-2015, 2015.

Matthew, B. M., Middlebrook, A. M., and Onasch, T. B.: Collection efficiencies in an Aerodyne Aerosol Mass Spectrometer as a function of particle phase for laboratory generated aerosols, Aerosol Sci. Technol., 42, 884-898, https://doi.org/10.1080/02786820802356797, 2008.

Middlebrook, A. M., Bahreini, R., Jimenez, J. L., and Canagaratna, M. R.: Evaluation of Composition-Dependent Collection Efficiencies for the Aerodyne Aerosol Mass Spectrometer using Field Data, Aerosol Sci. Technol., 46, 258-271, https://doi.org/10.1080/02786826.2011.620041, 2012.

Narukawa, M., Kawamura, K., Li, S. M., and Bottenheim, J. W.: Stable carbon isotopic ratios and ionic composition of the high-Arctic aerosols: An increase in delta C-13 values from winter to spring, J. Geophys. Res.: Atmos., 113, Artn D02312, https://doi.org/10.1029/2007jd008755, 2008.

Nguyen, Q. T., Skov, H., Sorensen, L. L., Jensen, B. J., Grube, A. G., Massling, A., Glasius, M., and Nojgaard, J. K.: Source apportionment of particles at Station Nord, North East Greenland during 2008-2010 using COPREM and PMF analysis, Atmos. Chem. Phys., 13, 35-49, https://doi.org/10.5194/acp-13-35-2013, 2013.

Nguyen, Q. T., Glasius, M., Sørensen, L. L., Jensen, B., Skov, H., Birmili, W., Wiedensohler, A., Kristensson, A., Nøjgaard, J. K., and Massling, A.: Seasonal variation of atmospheric particle number concentrations, new particle formation and atmospheric oxidation capacity at the high Arctic site Villum Research Station, Station Nord, Atmos. Chem. Phys., 16, 11319-11336, https://doi.org/10.5194/acp-16-11319-2016, 2016.

Onasch, T. B., Trimborn, A., Fortner, E. C., Jayne, J. T., Kok, G. L., Williams, L. R., Davidovits, P., and Worsnop, D. R.: Soot Particle Aerosol Mass Spectrometer: Development, Validation, and Initial Application, Aerosol Sci. Technol., 46, 804-817, https://doi.org/10.1080/02786826.2012.663948, 2012.

Orellana, M. V., Matrai, P. A., Leck, C., Rauschenberg, C. D., Lee, A. M., and Coz, E.: Marine microgels as a source of cloud condensation nuclei in the high Arctic, Proceedings of the National Academy of Sciences of the United States of America, 108, 13612-13617, https://doi.org/10.1073/pnas.1102457108, 2011.

Ovadnevaite, J., O'Dowd, C., Dall'Osto, M., Ceburnis, D., Worsnop, D. R., and Berresheim, H.: Detecting high contributions of primary organic matter to marine aerosol: A case study, Geophys. Res. Lett., 38, Artn L02807, https://doi.org/10.1029/2010gl046083, 2011.

Paatero, P., and Tapper, U.: Positive Matrix Factorization - a Nonnegative Factor Model with Optimal Utilization of Error-Estimates of Data Values, Environmetrics, 5, 111-126, https://doi.org/10.1002/env.3170050203, 1994.

Paatero, P.: Least squares formulation of robust non-negative factor analysis, Chemom. Intell. Lab. Syst., 37, 23-35, https://doi.org/10.1016/s0169-7439(96)00044-5, 1997.

Petzold, A., Kopp, C., and Niessner, R.: The dependence of the specific attenuation cross-section on black carbon mass fraction and particle size, Atmos. Environ., 31, 661-672, https://doi.org/10.1016/s1352-2310(96)00245-2, 1997.

Petzold, A., and Schonlinner, M.: Multi-angle absorption photometry - a new method for the measurement of aerosol light absorption and atmospheric black carbon, J. Aerosol Sci., 35, 421-441, https://doi.org/10.1016/j.jaerosci.2003.09.005, 2004.

Quinn, P. K., Miller, T. L., Bates, T. S., Ogren, J. A., Andrews, E., and Shaw, G. E.: A 3-year record of simultaneously measured aerosol chemical and optical properties at Barrow, Alaska, J. Geophys. Res.: Atmos., 107, Artn 4130, https://doi.org/10.1029/2001jd001248, 2002.

Quinn, P. K., Bates, T. S., Coffman, D., Onasch, T. B., Worsnop, D., Baynard, T., de Gouw, J. A., Goldan, P. D., Kuster, W. C., Williams, E., Roberts, J. M., Lerner, B., Stohl, A., Pettersson, A., and Lovejoy, E. R.: Impacts of sources and aging on submicrometer aerosol properties in the marine boundary layer across the Gulf of Maine, J. Geophys. Res.: Atmos., 111, Artn D23s36, https://doi.org/10.1029/2006jd007582, 2006.

Quinn, P. K., Shaw, G., Andrews, E., Dutton, E. G., Ruoho-Airola, T., and Gong, S. L.: Arctic haze: current trends and knowledge gaps, Tellus B, 59, 99-114, https://doi.org/10.1111/j.1600-0889.2006.00238.x, 2007.

Quinn, P. K., Bates, T. S., Baum, E., Doubleday, N., Fiore, A. M., Flanner, M., Fridlind, A., Garrett, T. J., Koch, D., Menon, S., Shindell, D., Stohl, A., and Warren, S. G.: Short-lived pollutants in the Arctic: their climate impact and possible mitigation strategies, Atmos. Chem. Phys., 8, 1723-1735, https://doi.org/10.5194/acp-8-1723-2008, 2008.

Quinn, P. K., Bates, T. S., Schulz, K., and Shaw, G. E.: Decadal trends in aerosol chemical composition at Barrow, Alaska: 1976-2008, Atmos. Chem. Phys., 9, 8883-8888, https://doi.org/10.5194/acp-9-8883-2009, 2009.

Rahn, K. A., and Heidam, N. Z.: Progress in Arctic Air Chemistry, 1977-1980 - a Comparison of the 1st and 2nd Symposia, Atmos. Environ., 15, 1345-1348, https://doi.org/10.1016/0004-6981(81)90339-5, 1981.

Saarnio, K., Teinila, K., Saarikoski, S., Carbone, S., Gilardoni, S., Timonen, H., Aurela, M., and Hillamo, R.: Online determination of levoglucosan in ambient aerosols with particle-into-liquid sampler - high-performance anion-exchange chromatography - mass spectrometry (PILS-HPAEC-MS), Atmos. Meas. Tech., 6, 2839-2849, https://doi.org/10.5194/amt-6-2839-2013, 2013.

Schmeisser, L., Backman, J., Ogren, J. A., Andrews, E., Asmi, E., Starkweather, S., Uttal, T., Fiebig, M., Sharma, S., Eleftheriadis, K., Vratolis, S., Bergin, M., Tunved, P., and Jefferson, A.: Seasonality of aerosol optical properties in the Arctic, Atmos. Chem. Phys., 18, 11599-11622, https://doi.org/10.5194/acp-18-11599-2018, 2018.

Sharma, S., Brook, J. R., Cachier, H., Chow, J., Gaudenzi, A., and Lu, G.: Light absorption and thermal measurements of black carbon in different regions of Canada, J. Geophys. Res.: Atmos., 107, 4771, https://doi.org/10.1029/2002JD002496, 2002.

Sharma, S., Lavoue, D., Cachier, H., Barrie, L. A., and Gong, S. L.: Long-term trends of the black carbon concentrations in the Canadian Arctic, J. Geophys. Res.: Atmos., 109, https://doi.org/10.1029/2003JD004331, 2004.

Sharma, S., Andrews, E., Barrie, L. A., Ogren, J. A., and Lavoue, D.: Variations and sources of the equivalent black carbon in the high Arctic revealed by long-term observations at Alert and Barrow: 1989-2003, J. Geophys. Res.: Atmos., 111, D14208, https://doi.org/10.1029/2005JD006581, 2006.

Sharma, S., Chan, E., Ishizawa, M., Toom-Sauntry, D., Gong, S. L., Li, S. M., Tarasick, D. W., Leaitch, W. R., Norman, A., Quinn, P. K., Bates, T. S., Levasseur, M., Barrie, L. A., and Maenhaut, W.: Influence of transport and ocean ice extent on biogenic aerosol sulfur in the Arctic atmosphere, J. Geophys. Res.: Atmos., 117, Artn D12209, https://doi.org/10.1029/2011jd017074, 2012.

Sharma, S., Ishizawa, M., Chan, D., Lavoue, D., Andrews, E., Eleftheriadis, K., and Maksyutov, S.: 16-year simulation of Arctic black carbon: Transport, source contribution, and sensitivity analysis on deposition, J. Geophys. Res.: Atmos., 118, 943-964, https://doi.org/10.1029/2012JD017774, 2013.

Shaw, P. M., Russell, L. M., Jefferson, A., and Quinn, P. K.: Arctic organic aerosol measurements show particles from mixed combustion in spring haze and from frost flowers in winter, Geophys. Res. Lett., 37, Artn L10803, https://doi.org/10.1029/2010gl042831, 2010.

Skov, H., Wahlin, P., Christensen, J., Heidam, N. Z., and Petersen, D.: Measurements of elements, sulphate and SO2 in Nuuk Greenland, Atmos. Environ., 40, 4775-4781, https://doi.org/10.1016/j.atmosenv.2006.03.057, 2006.

Skov, H., Massling, A., Nielsen, I. E., Nordstrøm, C., Bossi, R., Vorkamp, K., Christensen, J., Larsen, M. M., MHansen, K. M., Liisberg, J. B., and Poulsen, M. B.: AMAP core - atmospheric part: from 1990 to 2015. Results from Villum Research Station, Technical report no. 101, Aarhus University, DCE - Danish Centre for Environment and Energy, 2017.

Sodemann, H., Pommier, M., Arnold, S. R., Monks, S. A., Stebel, K., Burkhart, J. F., Hair, J. W., Diskin, G. S., Clerbaux, C., Coheur, P.-F., Hurtmans, D., Schlager, H., Blechschmidt, A.-M., Kristjánsson, J. E., and Stohl, A.: Episodes of cross-polar transport in the Arctic troposphere during July 2008 as seen from models, satellite, and aircraft observations, Atmos. Chem. Phys., 11, 3631-3651, https://doi.org/10.5194/acp-11-3631-2011, 2011.

Stohl, A.: Characteristics of atmospheric transport into the Arctic troposphere, J. Geophys. Res.: Atmos., 111, Artn D11306, https://doi.org/10.1029/2005jd006888, 2006.

Stohl, A., Berg, T., Burkhart, J. F., Fjæraa, A. M., Forster, C., Herber, A., Hov, Ø., Lunder, C., McMillan, W. W., Oltmans, S., Shiobara, M., Simpson, D., Solberg, S., Stebel, K., Ström, J., Tørseth, K., Treffeisen, R., Virkkunen, K., and Yttri, K. E.: Arctic smoke - record high air pollution levels in the European Arctic due to agricultural fires in Eastern Europe in spring 2006, Atmos. Chem. Phys., 7, 511-534, https://doi.org/10.5194/acp-7-511-2007, 2007.

Stohl, A., Klimont, Z., Eckhardt, S., Kupiainen, K., Shevchenko, V. P., Kopeikin, V. M., and Novigatsky, A. N.: Black carbon in the Arctic: the underestimated role of gas flaring and residential combustion emissions, Atmos. Chem. Phys., 13, 8833-8855, https://doi.org/10.5194/acp-13-8833-2013, 2013.

Stroeve, J., Holland, M. M., Meier, W., Scambos, T., and Serreze, M.: Arctic sea ice decline: Faster than forecast, Geophys. Res. Lett., 34, L09501, https://doi.org/10.1029/2007gl029703, 2007.

Tunved, P., Strom, J., and Krejci, R.: Arctic aerosol life cycle: linking aerosol size distributions observed between 2000 and 2010 with air mass transport and precipitation at Zeppelin station, Ny-Alesund, Svalbard, Atmos. Chem. Phys., 13, 3643-3660, https://doi.org/10.5194/acp-13-3643-2013, 2013.

Twomey, S.: The influence of pollution on the shortwave albedo of clouds, J. Atmos. Sci., 34, 1149-1152, https://doi.org/10.1175/1520-0469(1977)034<1149:TIOPOT>2.0.CO;2, 1977.

Udisti, R., Bazzano, A., Becagli, S., Bolzacchini, E., Caiazzo, L., Cappelletti, D., Ferrero, L., Frosini, D., Giardi, F., Grotti, M., Lupi, A., Malandrino, M., Mazzola, M., Moroni, B., Severi, M., Traversi, R., Viola, A., and Vitale, V.: Sulfate source apportionment in the Ny-Alesund (Svalbard Islands) Arctic aerosol, Rend Lincei-Sci Fis, 27, 85-94, https://doi.org/10.1007/s12210-016-0517-7, 2016.

Ulbrich, I. M., Canagaratna, M. R., Zhang, Q., Worsnop, D. R., and Jimenez, J. L.: Interpretation of organic components from Positive Matrix Factorization of aerosol mass spectrometric data, Atmos. Chem. Phys., 9, 2891-2918, https://doi.org/10.5194/acp-9-2891-2009, 2009.

Willis, M. D., Leaitch, W. R., and Abbatt, J. P. D.: Processes Controlling the Composition and Abundance of Arctic Aerosol, Rev. Geophys., 56, https://doi.org/doi:10.1029/2018RG000602, 2018.

Winiger, P., Andersson, A., Yttri, K. E., Tunved, P., and Gustafsson, O.: Isotope-Based Source Apportionment of EC Aerosol Particles during Winter High-Pollution Events at the Zeppelin Observatory, Svalbard, Environ. Sci. Technol., 49, 11959-11966, https://doi.org/10.1021/acs.est.5b02644, 2015.

Zangrando, R., Barbaro, E., Zennaro, P., Rossi, S., Kehrwald, N. M., Gabrieli, J., Barbante, C., and Gambaro, A.: Molecular Markers of Biomass Burning in Arctic Aerosols, Environ. Sci. Technol., 47, 8565-8574, https://doi.org/10.1021/es400125r, 2013.

Zhang, Q., Alfarra, M. R., Worsnop, D. R., Allan, J. D., Coe, H., Canagaratna, M. R., and Jimenez, J. L.: Deconvolution and quantification of hydrocarbon-like and oxygenated organic aerosols based on aerosol mass spectrometry, Environ. Sci. Technol., 39, 4938-4952, https://doi.org/10.1021/es048568l, 2005.

Zhang, Q., Jimenez, J. L., Canagaratna, M. R., Ulbrich, I. M., Ng, N. L., Worsnop, D. R., and Sun, Y.: Understanding atmospheric organic aerosols via factor analysis of aerosol mass spectrometry: a review, Anal. Bioanal. Chem., 401, 3045-3067, https://doi.org/10.1007/s00216-011-5355-y, 2011.

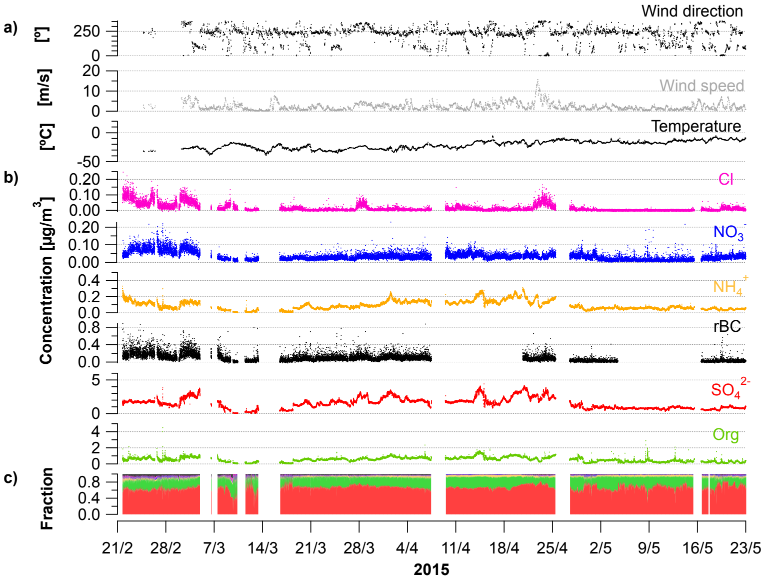

Figure 1 Time series from 21 February to 23 May 2015 showing a) wind direction [°], mean wind speed [m/s] and temperature [°C], b) concentrations of Cl, NO_3^-, NH_4^+, rBC, SO_4^{2-} and OA from the SP-AMS [µg/m³], and c) fraction of the aerosol species to the total PM_1.

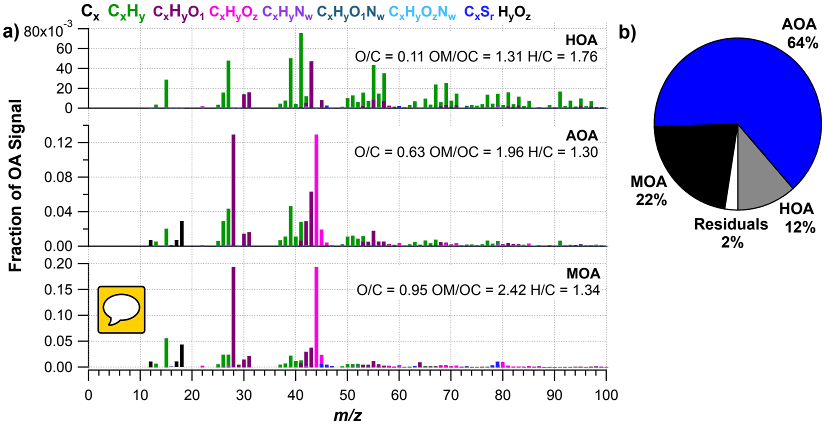

Figure 2 a) High-resolution mass spectra of PMF factors hydrocarbon-like organic aerosol (HOA), Arctic haze organic aerosol (AOA) and marine organic aerosol (MOA), and b) factor share of ambient mass concentration. O/C, OM/OC and H/C ratio are presented for each factor.

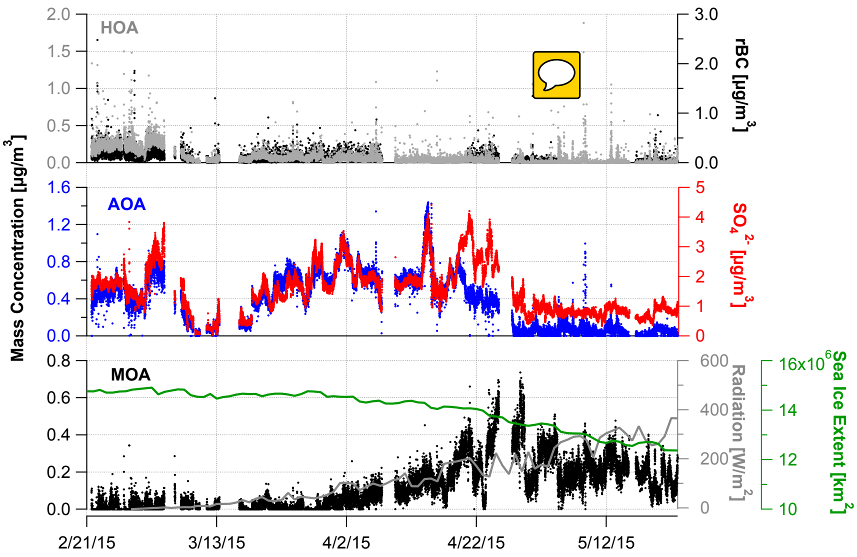

Figure 3 Time series for hydrocarbon-like organic aerosol (HOA), Arctic haze organic aerosol (AOA), marine organic aerosol (MOA) and tracers (rBC, SO$_4^{2-}$). Sea ice extension on the Northern hemisphere and short-wave radiation (daily average) are included in the time series for MOA (see text).

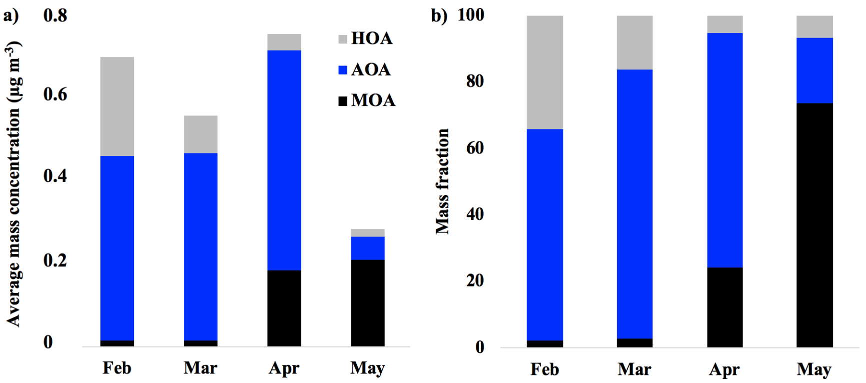

Figure 4 a) average mass concentration (µg m^{-3}) of hydrocarbon-like organic aerosol (HOA), Arctic haze organic aerosol (AOA) and marine organic aerosol (MOA) in February, March, April and May. b) mass fraction of HOA, AOA and MOA in February, March, April and May.

Table 1 Detection limits. The detection limits for the SP-AMS is calculated from periods sampling through HEPA filters with a time resolution of 2 minutes (average from eight hepafilter periods of 30 to 60 minutes over the entire campaign). The detection limit for the MAAP is from Massling et al. (2015).

Instruments	Species	Lower Detection Limit
AMS	HR Org	0.131 μg/m^3
	HR SO_4^{2-}	0.024 μg/m^3
	HR NO_3^-	0.021 μg/m^3
	HR NH_4^+	0.006 μg/m^3
	HR Cl	0.014 μg/m^3
	HR rBC	0.010 μg/m^3
MAAP	BC	< 0.006 μg/ m^3

Table 2 R^2 correlations between PMF factors and tracers (rBC, MSA, SO_4^{2-} and NH_4^+).

	HOA	**AOA**	**MOA**	**rBC**	**MSA**	**SO_4^{2-}**	**NH_4^+**
HOA	-	**0.08**	**0.11**	**0.35**	**0.13**	**0.08**	**0.04**
AOA	-	-	**0.14**	**0.21**	**0.27**	**0.67**	**0.49**
MOA	-	-	-	**0.07**	**0.68**	**0.00**	**0.03**
rBC	-	-	-	-	**0.08**	**0.18**	**0.15**
MSA	-	-	-	-	-	**0.02**	**0.00**
SO_4^{2-}	-	-	-	-	-	-	**0.70**
NH_4^+	-	-	-	-	-	-	-